RESEARCH ARTICLE

CJ CE | THE CANADIAN JOURNAL OF CHEMICAL ENGINEERING

Distribution of potassium during chemical activation of petroleum coke: Electron microscopy evidence and links to phase behaviour

Vicente Montes[1] [ID] | **Ye Xiao**[2] | **Jingfeng Wu**[2] | **Josephine M. Hill**[2] [ID]

[1]Department of Chemical Engineering and Physics Chemistry, University Institute of Research in Water, Climate Change and Sustainability (IACYS), University of Extremadura, Badajoz, Spain

[2]Department of Chemical and Petroleum Engineering, University of Calgary, Calgary, Alberta, Canada

Correspondence
Vicente Montes, Department of Chemical Engineering and Physics Chemistry, University Institute of Research in Water, Climate Change and Sustainability (IACYS), University of Extremadura, Badajoz, Spain.
Email: vmontes@unex.es

Abstract

In this study, direct evidence for chemical penetration into petroleum coke particles during activation is presented. In addition, the porosity development was directly related to the sulphur loss and phase behaviour of the species present. Petroleum coke (petcoke, 6 wt.% sulphur) was activated with KOH and NaOH at temperatures between 400 and 800°C. The C—S bonds were broken before 400°C in the presence of KOH and before 500°C in the presence of NaOH. Electron microscopy analysis of cross-sectioned and ultramicrotomed samples revealed that sulphur was still present within the particles and that the hydroxide activation agents had penetrated to the centre of the particles (90–150 μm). After heating to 800°C and washing with a weak acid aqueous solution, essentially all the sulphur was removed, as was any remaining chemical agent. The characterization results, phase diagrams, and complementary experiments with carbonate chemical agents or steam suggest that, during heating, a molten phase formed around the petcoke particles. The composition of this molten phase changed as activation proceeded and both sulphur and ash components were liberated from the petcoke. This better understanding of the activation process will improve the efficiency of preparing activated carbon.

KEYWORDS
activated carbon, chemical activation, desulphurization, petroleum coke, potassium hydroxide

1 | INTRODUCTION

Since the chemical activation of carbon by potassium hydroxide was patented in 1978 by Wennerberg and O'Grady,[1] many publications have reported the preparation of activated carbon (AC) with alkali species, especially KOH or NaOH.[2–6] Some of the main challenges with chemical activation are low yield, high temperature, and emissions or residues. A better understanding of the activation process could result in higher efficiency processes (i.e., higher yields and lower activation temperatures) that can be applied to a wide range of carbon sources. Petroleum coke (petcoke) is one of the waste carbon materials that has been extensively studied to

prepare AC.[7–11] A byproduct of the upgrading of heavy oil and bitumen, petcoke is mainly (>80 wt.%) fixed carbon but contains many other elements, including sulphur (up to ~7 wt.%) in the form of thiophene (50–55 wt.%), sulphides or sulphoxides (25–35 wt.%), or sulphates (10–20 wt.%).[12–14] The C—S bond is weaker than the C—C bond, and is broken first during chemical activation, as shown by Lee and Choi through FTIR analysis.[15] During and/or after activation, sulphur species have been detected in the gas phase as H_2S and SO_2 and in the solid phase as sulphates and M_2S.[13] The influence of sulphur on porosity developed during chemical activation has not been deeply explored.

Pore development has been ascribed to various mechanisms, including gasification and intercalation.[16] During gasification, carbon and hydroxide species (MOH, where M may be K, Na, or other alkali metals) are converted to gas, carbonate, and metallic species. The hydroxide ions (OH—) interact with the carbon (C), forming C—OH, C=O, or C—O—C groups,[3,5] which can increase the reactivity on the external layers of the petcoke particles. The following reactions are commonly provided as the overall reactions.[17–20]

$$6MOH + 2C \rightarrow 2M + 3H_2 + 2M_2CO_3 \qquad (1)$$

$$6MOH + 4C \rightarrow 4M + 3H_2 + M_2CO_3 + 3CO \qquad (2)$$
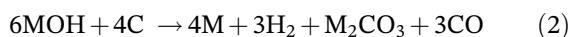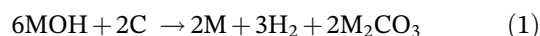
The activation process, however, is complex and involves many other reactions and processes. The intercalation of the metallic alkali species into the carbon matrix has been proposed during heating based on indirect evidence, including hydrogen production or an increase (from 0.35 to 0.4 nm) in graphite d_{002} spacing.[21,22] Xu and colleagues[21] extracted potassium from petcoke activated with KOH and calculated that the amount of K metal in situ (intercalated) was similar to that in a free state (gas phase) and equal to over 50% of the KOH added. A study with pure graphite showed that the intercalation of potassium into graphite is minimal.[23] Although the process of potassium intercalation into petcoke is not clear, these studies demonstrate that KOH dissociates during activation and the potassium diffuses into the particles to some extent.

Carbonate species (e.g., K_2CO_3 or Na_2CO_3) are the main species (~80 mol.%) detected after cooling AC,[12,18,24] but these species are both inactive relative to hydroxide species[25] and not favoured thermodynamically at activation temperatures. For example, at 700°C, a mixture of K_2O and K in a ratio of 4:1 is predicted with minimal amounts of K_2CO_3.[18] Our previous work[26] suggested that the petcoke was surrounded by a molten phase, consistent with the phase diagram for potassium,

which indicated that the species would be in a liquid state at 800°C.[27] The current study builds on this result to demonstrate the distribution of the chemical species throughout the petcoke particles during activation and link the phase behaviour to the activation process.

More specifically, delayed petcoke containing ~6 wt. % sulphur was activated with KOH and NaOH at 400–800°C in N_2. Experiments with K_2CO_3 and Na_2CO_3, which have different fusion temperatures than KOH and NaOH, and with steam addition, which increases the porosity,[28] were also done. The AC products were characterized with nitrogen adsorption (for surface area, porosity, and pore size distribution determination), elemental analysis, and scanning and transmission electron microscopy (cross-sectioned samples for morphology and composition analysis).

2 | EXPERIMENTAL

2.1 | Materials

The following chemicals were used in this study: KOH flakes (85%), HNO_3 (68%–70%), and HCl (36.5%–38%) purchased from VWR International (Pennsylvania, USA); NaOH pellets (97%), Na_2CO_3 (>97%), and K_2CO_3 pellets (>97%) purchased from Sigma Aldrich, Missouri, USA. Delayed petcoke (Alberta, Canada) was ground and sieved to a size range of 90–150 μm. Briefly, the petcoke contains 87 wt.% fixed carbon, 10 wt.% volatile species, 6 wt.% sulphur, and 3 wt.% ash. The structure of petcoke is heterogeneous with a mixture of graphitic and amorphous phases. More details on the composition have been reported elsewhere.[29,30]

2.2 | Chemical activation

Chemical activation consisted of mixing 2.5 g of ground petcoke (90–150 μm, which is typical of the particle size used in activation of petcoke and biomass) with the chemical agent—KOH, NaOH, K_2CO_3, or Na_2CO_3—in the desired chemical agent to carbon ratio (mass ratios from 0.5 to 5) in a mortar until the solid mixture was homogeneous (to the eye). The mixture was then put in a ceramic boat of 20 cm^3 and placed in the centre of a furnace. The activation procedure consisted of increasing the temperature to 400, 500, 600, or 800°C at a rate of 5°C/min under N_2 flow (250 cm^3/min). Once at the desired temperature, the heating was stopped, and the sample cooled to room temperature before being removed from the ceramic boat with deionized water and filtered in a Buchner filter. The sample was washed in

the filter with 250 cm³ of 1 M HCl solution followed by deionized water until the pH of the rinse water was neutral. Finally, the sample was dried at 150°C overnight. Experiments with steam activation followed the same procedure, except that the sample was exposed to humidified N_2 (50 cm³/min N_2 plus 5 cm³/h liquid water) at 800°C for 30 min.

The solid product of all experiments will be referred to as AC. The yield of AC was calculated by dividing the mass of AC by the initial mass of petcoke:

$$\text{Yield}(\%) = \frac{\text{Mass of AC}}{\text{Initial mass of petcoke}} \times 100\% \qquad (3)$$

The nomenclature for the samples is as follows; P (indicating petcoke), followed by the chemical agent to carbon mass ratio, chemical agent, and maximum temperature (°C). For example, P1KOH800 refers to a 1:1 KOH to carbon mixture activated by heating to 800°C. Samples activated with steam have the suffix '/St'.

2.3 | Sample characterization

Porous structure analysis was done by N_2 physisorption at 77 K (TriStar II Plus, Micromeritics, Atlanta, USA). Before analysis, all samples were degassed at 150°C for 5 h. Pore volume was determined by the quantity of gas adsorbed at a relative partial pressure (P/P_0) of 0.97. Non-local density functional theory (NLDFT) models were used to determine the pore size distribution and surface area using Solution of the Adsorption Integral Equation Using Splines (SAIEUS) software (Micromeritics, Atlanta, USA). Specifically, the two-dimensional NLDFT with heterogeneous surface (2D-NLDFT-HS) model was used for the isotherms of samples activated with KOH, and the 2D-NLDFT (aspect ratio, As = 6) model was used for isotherms of samples activated with NaOH. The isotherms of the other samples (i.e., those prepared with carbonate precursors) were fit with the NLDFT model. Different methods were used according to the best fit for each isotherm. More details on these methods and their applications to carbon-based materials are available elsewhere.[31]

CO_2 adsorption at 0°C is appropriate for accessing and quantifying micropores of less than 1.4 nm. CO_2 adsorption was done at 0°C using an ice bath on the TriStar II Plus adsorption instrument. Before analysis, all samples were degassed at 150°C for 5 h. The CO_2 adsorption isotherm was fit with the 2D-NLDFT-HS model using the SAIEUS software to obtain the pore structure information.

Scanning electron microscopy (SEM) images were acquired using an environmental SEM (FEI Quanta 250 FEG, FEI, Hillsboro, USA) with a power of 20 kV and a desktop SEM-energy dispersive X-ray (SEM–EDX,
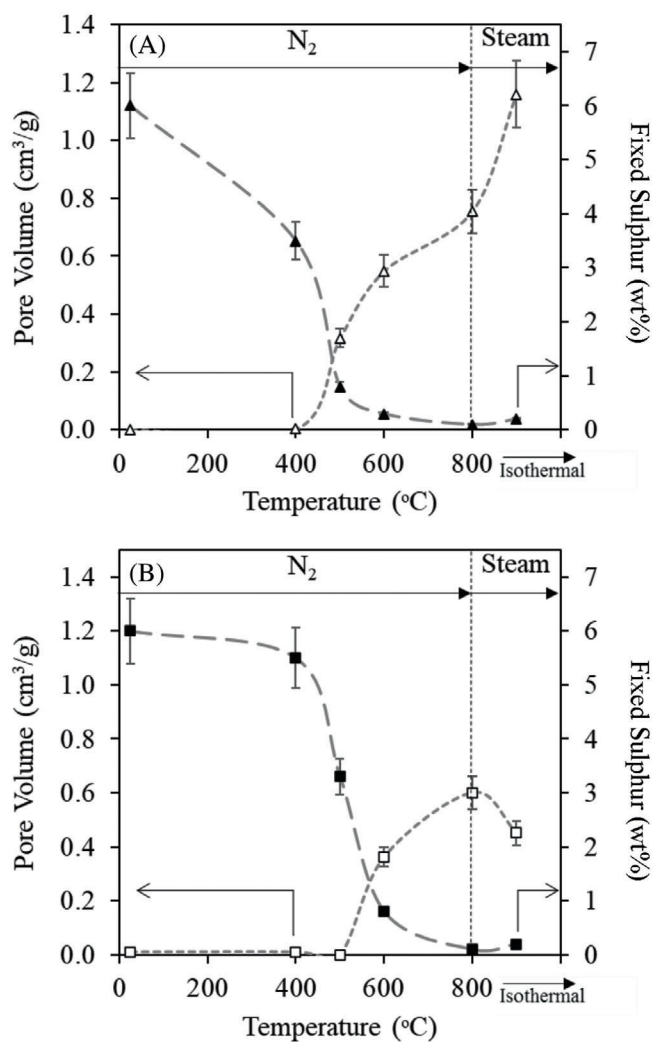

FIGURE 1 Impact of temperature on resulting pore volume (open symbols, left axis) and fixed sulphur content (filled symbols, right axis) of petcoke activated with (A) KOH (▲,△) and (B) NaOH (■,□); MOH to carbon ratio of 2 with heating under N_2 flow to the given temperature or for the right most points, heating under N_2 flow to 800°C followed by 30 min of steam exposure

Phenom ProX, Eindhoven, Netherlands) with a power of 15 kV. Particle size distributions were determined using ImageJ® software. Samples were placed on a holder using carbon tape and then imaged. For sample cross-sections, selected samples were embedded in an epoxy resin (Devcon, USA) by mixing approximately three parts of resin with one part of sample by volume. A glass Pasteur pipette (0.75 cm internal diameter) was filled with the mixture. After the resin solidified (overnight), the pipette was dipped into liquid N_2 to remove the glass pipette. The resin was fractured to expose the embedded sample, which was then mounted on carbon tape and analysed in the SEM (FEI Quanta 250 FEG). Some of the unwashed samples were polished (7.5 N, 15–50 rpm, Stuers PDM Force 20 and Roto Pol, Denmark) before analysis in the SEM. A transmission electron microscope (TEM, Jeol

TABLE 1 Physical properties and sulphur contents of petcoke and activated carbon (AC) produced at various conditions

Chemical agent	Mass ratio	Molar ratio	Atmosphere	Temperature[a] (°C)	Pore volume (cm³/g)	Surface area (m²/g)	Sulphur content (wt.%)	Yield (%)
None	-	-	N_2	800	<0.01	<0.1	6.5	98
KOH	2	0.43	N_2	400	<0.01	<1	3.5[c]	96
KOH	2	0.43	N_2	500	0.31	870	0.8	86
KOH	2	0.43	N_2	600	0.55	1358	0.3	75
KOH	2	0.43	N_2	800	0.68	1867	0.3[c]	76
KOH	2	0.43	N_2 + Steam[b]	800	1.08	1576	0.1	47
KOH	0.5	0.11	N_2	800	0.2	379	0.8[c]	82
KOH	1	0.21	N_2	800	0.38	845	0.5	80
KOH	3	0.64	N_2	800	1.01	1940	0.3	72
KOH	5	1.07	N_2	800	1.35	2438	0.1	66
K_2CO_3	0.7	0.11	N_2	800	0.19	387	1.1	86
K_2CO_3	1.3	0.21	N_2	800	0.26	521	0.8	82
K_2CO_3	2.6	0.43	N_2	800	0.26	541	0.9	71
K_2CO_3	3.9	0.64	N_2	800	0.27	567	0.9	67
K_2CO_3	6.5	1.07	N_2	800	0.26	534	0.7	58
Na_2CO_3	2	0.43	N_2	800	<0.01	14	6.0	97
NaOH	2	0.71	N_2	400	0.01	<1	5.5	99
NaOH	2	0.71	N_2	500	0.36	680	3.6	82
NaOH	2	0.71	N_2	800	0.6	1034	0.3	65
NaOH	2	0.71	N_2 + Steam[b]	800	0.45	560	0.4	45
NaOH	0.5	0.18	N_2	800	0.05	<1	0.8	94
NaOH	1	0.35	N_2	800	0.19	396	0.5	76
NaOH	3	1.06	N_2	800	0.8	1277	0.3	56

[a]Once this temperature was reached, the furnace was shut off so that the sample immediately began to cool.

[b]Once 800°C was reached, steam was added to the nitrogen flow and the sample was held in this condition for 30 min before the furnace was shut off.

[c]Sulphur content verified with ICP.

JEM 1400, Tokyo, Japan) was used to collect high-resolution images. The samples were embedded in epoxy resin and cut in slices ~150 nm thick using an ultramicotome (LEICA-ULTRACUT R, Barcelona, Spain).

The bulk elemental composition (C, N, S, O) of samples was determined using an elemental Truspec Micro from Leco (Leco Instruments, Madrid, Spain) with 2 mg of sample using infrared (IR) and thermal conductivity detectors (TCD). Inductively coupled plasma-optical emission spectrometry (ICP-OES, ThermoFisher Scientific IRIS Intrepid IIXDL, Waltham, USA) was used to obtain the sulphur and potassium concentrations in the washing solutions and water trap after the activation of a few samples to confirm the mass balances.

The properties of the chemical reagents used for the calculation of cation volume (M density at 800°C, and theoretical yield [carbon density of 2 g/cm³]) are listed in Table S1, with values obtained from the work of Foust.[32]

The densities of the petcoke and some AC samples were measured by immersing ~0.5 g of sample into 5 ml of isopropanol in a graduated cylinder. The cylinder was covered by Parafilm and allowed to equilibrate overnight. The total volume of sample and isopropanol was then recorded to calculate the density.

3 | RESULTS AND DISCUSSION

3.1 | Porosity and sulphur content

Heating petcoke without any activation agent did not change its surface area or sulphur content. After activation with KOH, essentially no porosity developed until the temperature reached ~400°C (Figure 1A). At these temperatures, the sulphur content had decreased from ~6 to ~3.5 wt.%. The term 'fixed sulphur' was used on

the graph (right axis in Figure 1) because the sulphur content was determined after cooling and washing the sample. Throughout the remainder of this paper 'sulphur content' refers to the fixed sulphur remaining in the samples. As the final temperature was increased to 800°C, the pore volumes increased to 0.68 cm^3/g. Because the heating rate was constant (5°C/min), the total activation time increased as the final temperature increased. Experiments with the same total activation time at each temperature confirmed that the additional activation observed at the higher temperatures was a result of the temperature and not the increased activation time. Activation of petcoke with NaOH (Figure 1B) followed a similar trend to that with KOH (Figure 1A) but porosity developed at a temperature ~100°C higher and the resulting AC had a lower pore volume (0.60 cm^3/g).

With increasing activation temperature, the sulphur content continued to decrease to below 0.5 wt.% (less than 10% of the original sulphur [Table 1 and Figure 1]). Changing the KOH to carbon mass ratio from 0.5 to 5, with activation at 800°C, increased the porosities obtained from 0.2 to 1.35 cm^3/g, and decreased the yields from 82% to 66%, but with all ratios, the sulphur contents were less than 1 wt.% after activation, and as low as 0.1 wt.% with the highest KOH to carbon ratio (Table 1). The trends were the same for activation with NaOH, but KOH was a more effective activation agent in terms of pore development, despite the molar ratios being higher for NaOH. The results are as expected and similar to those reported previously in the literature.[13,33,34] Namely, the yield decreased while the surface area and pore volume increased with increasing activation temperature; more porosity was obtained with KOH than with NaOH; and the addition of steam increased the pore sizes but decreased the yield.

The N$_2$ adsorption isotherm was Type I with little to no hysteresis loop for petcoke activated with KOH; over 94% of the pores were micropores (Figure S1a,c). The addition of steam at 800°C increased the pore volume to 1.1 cm^3/g and increased the mean pore size such that there was a second peak in the pore size distribution at ~2 nm; 71% of the pores were microporous (Figure S1c). Activation with NaOH produced slightly larger pores than with KOH, with a mean pore size of 2.0 nm (76% micropores) and a broader pore size distribution up to ~30 nm; the adsorption isotherm was Type I with a hysteresis loop indicative of different-sized pores with a bottle shape (Figures S1b,d and S2). Hysteresis loops obtained at different partial pressures (Figure S2a) resulted in the same Type I isotherms regardless of the activation temperature. This result provides evidence that the shape of the pores did not evolve over time. The addition of steam, however, reduced and/or widened the

micropores.[26] These changes resulted in decreases in the pore volume to 0.45 cm^3/g and the yield to 45% (Table 1).

The TEM images of ultramicrotomed petcoke before and after activation with KOH are shown in Figures 2 and S3. The microtoming did not cleanly cut the samples, resulting in some surface roughness. The higher magnification images were obtained from the centre of the particles, as shown by the circles in Figure 2A,C,E. The images of the petcoke particles (Figure 2A,B) contain dark spots corresponding to the inorganic contaminants (i.e., ash). After activation, the ash was removed by washing. The porous structure is irregular and consists mainly of micropores, consistent with the results of the N$_2$ adsorption analysis (Table 1 and Figure S1). The AC particles (Figures 2C–F and S3e–f) exhibit more fractures and more nano-porosity than the petcoke particles. These images are the first to show the porous structure within an AC particle (90–150 μm).

The other contribution to pore volume creation may be the exposure of occluded pores during activation, especially at temperatures below 600°C (i.e., after the sulphur released). The density of the petcoke was 1.26 g/cm^3, which is less than that of graphite (2.26 g/cm^3), and it increased to 1.60 g/cm^3 after activation at 600°C, consistent with some pores becoming accessible to the isopropanol (kinetic diameter of 0.47 nm),[35] used to measure the density. This increase in density suggests that occluded pores in the petcoke contribute to the pore development.

Regardless of the activation conditions (i.e., temperature, amount and/or type of chemical agent), pore volume higher than 0.1 cm^3/g was not created until the sulphur content was lower than 1 wt.%, as shown in Figures 1 and S4 (in which the sulphur content is plotted versus the pore volume for all activation conditions). With the lowest amount of chemical agent used (i.e., mass ratio of chemical agent to carbon of 0.5), the number of moles of either KOH or NaOH was more than five times the number of moles of sulphur; thus, the chemical agent was not limiting the formation of M$_2$S or M$_2$SO$_4$ (where M refers to K or Na). Although sulphur species transformation is accepted as the first step in pore development, the study herein relates the sulphur loss to porosity creation and examines the sulphur distribution within the activated samples (discussion below).

3.2 | Penetration of potassium and distribution of sulphur

SEM analysis of cross-sections of the raw petcoke (Figures 3A–C, and S5a,b) showed the homogeneous distribution of sulphur and a lack of micron size porosity throughout the particles. Heating to 800°C with no
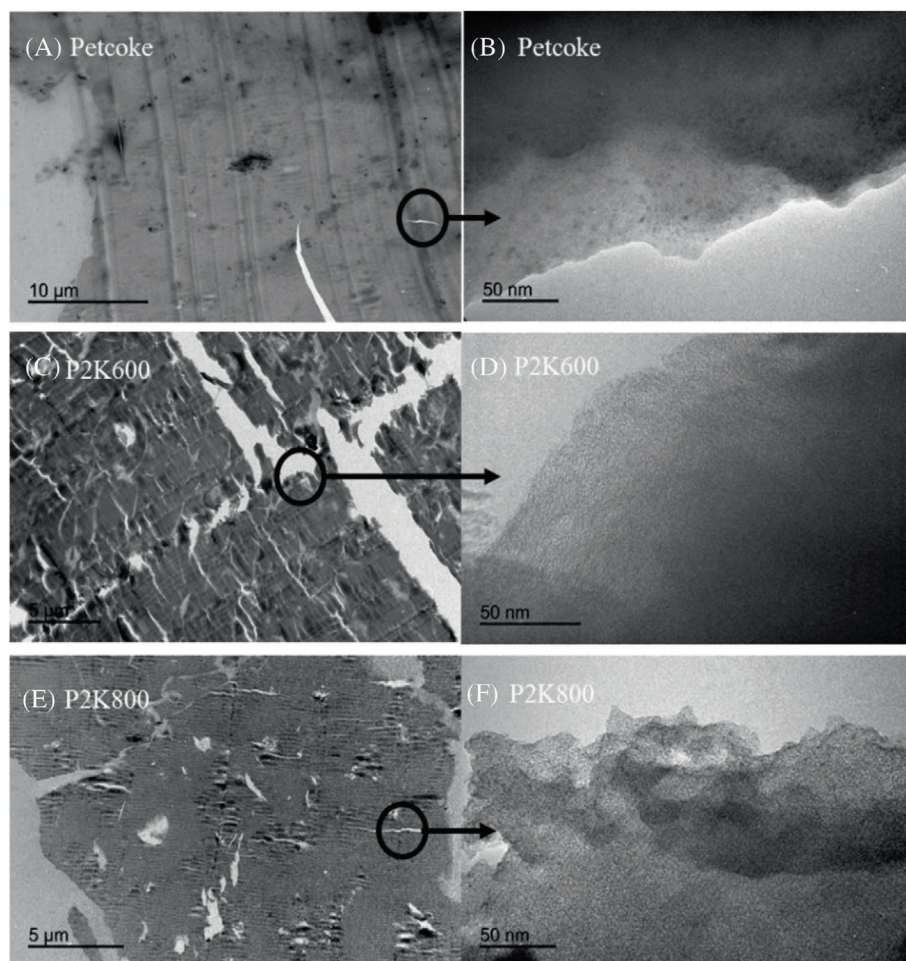
FIGURE 2 Transmission electron microscope (TEM) images of ultramicrotomed particles taken at (A, B) the core of petcoke, (C, D) activated carbon (AC) with KOH at 600°C, and (E, F) AC with KOH at 800°C. Chemical reagent to carbon mass ratio of 2

chemical agent did not change the sulphur content of pet-coke (images not shown), consistent with the results summarized in a review of coke and anode desulphurization by Edwards et al.[36] After activation with KOH at 500°C, the AC still had a homogeneous distribution of sulphur (Figure 3D,E), but the sulphur content had decreased to 0.9 wt.%. After activation at 800°C, the sulphur content decreased further to ∼0.3 wt.% (Figures 3 and S5, respectively) and macropores were visible. Changing the amount of chemical agent had a minor effect on the change in sulphur content: with mass ratios of 0.5, 1, 2, and 3, the sulphur contents after activation were 0.9 wt.%, 0.5 wt.%, 0.3 wt.%, and 0.3 wt.%, respectively (Table 1, Figure S6).

As most of the sulphur was released by heating to 800°C with KOH, exposure to steam for an additional 30 min at 800°C did not change the amount of sulphur significantly. The morphology of this sample, however, was significantly different (Figures 3I,K and S7), and the particles were expanded throughout, suggesting that the porosity developed by 800°C facilitated the diffusion of the steam to the core of the particles.

Activation with NaOH also reduced the sulphur content to 0.3 wt.% (Figure S5) and resulted in macropores.

After activation with KOH (Figure 3H), however, the pores have a higher aspect ratio (i.e., length to diameter) and are more frequent than those developed with NaOH (Figure S5i) for the same activation conditions. The particle sizes were generally much smaller after activation (compare particle sizes in Figure S5, in which the AC particles are approximately half the size of the petcoke particles), suggesting that some of the petcoke particles cracked and/or gasified during activation.

In physical activation and gasification of petcoke with CO_2, there were differences in the nitrogen uptakes for different particle sizes (20–45 to 300–600 μm)[31] consistent with porosity developing from the outside of the particle inwards—the so-called shrinking core model.[37] For the samples generated in this study with chemical activation, there were no differences in the nitrogen uptakes for particles of different sizes from <20 μm (obtained by ball-milling and sieving the samples after activation) to 150 μm, indicating the pores were created within the particles, and not from the outside in. To further verify this result, very large (>10 000 μm) petcoke particles were activated with KOH or NaOH at 800°C with a heating rate of 10°C/min. After activation, the pore volumes were

FIGURE 3 Scanning electron microscopy (SEM) images and sulphur mapping of cross-sectioned particles of (A–C) petcoke, (D, E) activated carbon (AC) with KOH in a chemical reagent to carbon mass ratio of 2 at 500°C, (F–H) 800°C, and (I–K) 800°C after 30 min steam exposure
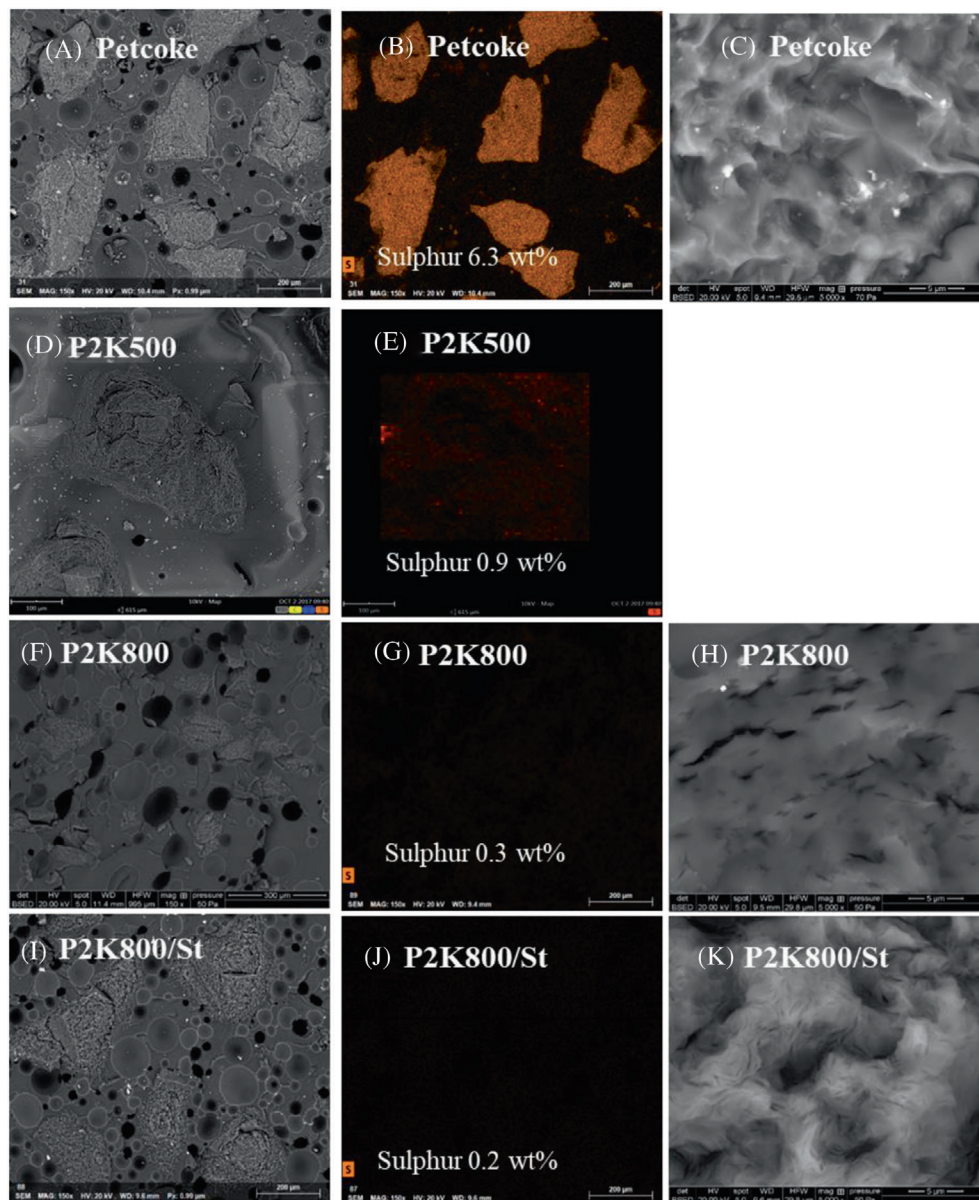
uniform throughout the particles, suggesting that the rates of potassium and sodium diffusion through the petcoke were faster than 2000 µm/min (calculated using the radius of the biggest particle tested [5000 µm] and 40 min of activation, from 400 to 800°C).

The samples analyzed in Figure 3 had been washed, which removed the chemical agent. Analysis of unwashed samples was attempted to see the distribution of chemical agent in the particles. Without washing, the particles stayed intact when fracturing the resin, so no cross-sections were exposed (Figure 4). The particles were coated with either potassium or sodium, and sulphur and aluminum were also present on the exterior of the particles. Sulphur was relatively uniformly distributed after activation with KOH, but accumulated in nanorod structures after activation with NaOH. According to

SEM/EDX analysis, the nanorods contained only Na and S. The difference in sulphur distribution after activation with the two chemical agents may be a consequence of the different fusion temperatures for the alkali metal sulphides that could form. That is, the fusion temperature of K_2S is 740°C and below the activation temperature of 800°C, while that of Na_2S is 1176°C and above the activation temperature. If formed, K_2S would be molten and able to disperse on the surface of the particle, while Na_2S would be solid and have limited mobility.

A second attempt was made to access particle cross-sections by polishing the fractured resin surface of AC prepared with KOH. In this method, some of the chemical agent was preferentially polished away and/or dissolved in the oil solution used for polishing, and so quantitative analysis was not possible. Even if some of
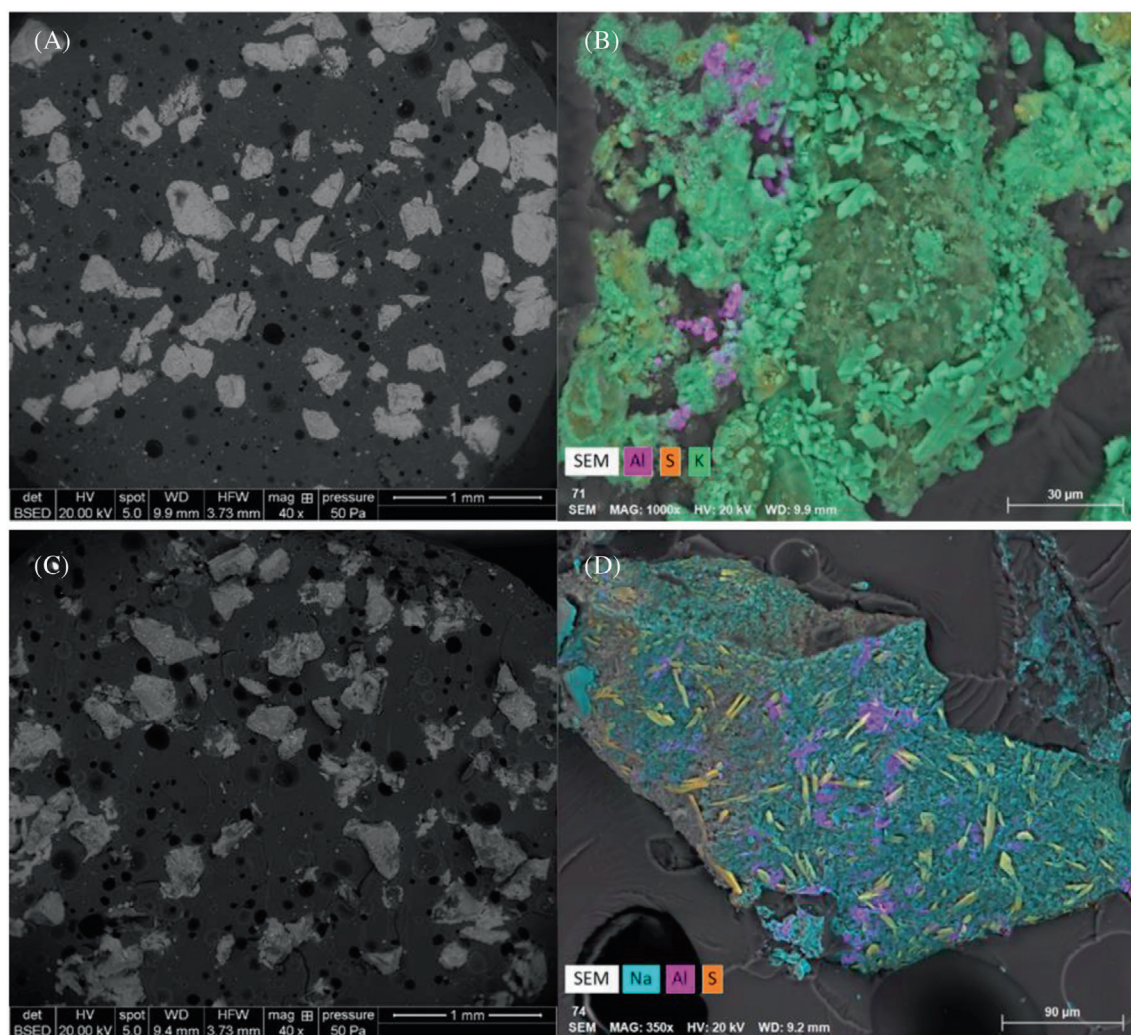
FIGURE 4 Scanning electron microscopy (SEM) images and potassium, sodium, and sulphur mapping of AC from petcoke activated with (A, B) KOH and (C, D) NaOH in a chemical agent to carbon mass ratio of 2 at 800°C without the washing step

the chemical agent was removed during the SEM sample preparation, the images show that both K and S were distributed throughout the particles (Figure 5). These results confirmed that the potassium reached the centre of the petcoke particles and that sulphur was present throughout particles before washing. In the experiments herein, gas phase sulphur species were collected in a scrubber solution of H_2O downstream of the reactor. The sulphur balance closed when summing the sulphur remaining on the unwashed samples, or in the washing solution from the washed samples—∼70 wt.%, and that collected in the scrubber—∼30 wt.%. The sulphur distribution is similar to that reported by Shan et al.[12] for the activation of petcoke (∼4 wt.% S) with KOH at 800°C.

Activation with steam provided further evidence that K and Na migrated throughout the petcoke particles (90–150 μm), as seen in SEM images of cross-sectioned samples in Figures 3 and S7. Without initial porosity (i.e., pores larger than those accessible to CO_2), the steam

cannot penetrate into the particles.[31] While K and Na create porosity, these species also catalyze steam gasification, resulting in significantly decreased yields (<50%, Table 1).

3.3 | Pore development and chemical phase behaviour

It is established that hydroxide species are better activation agents than carbonate species.[25] As shown in Table 1, the porosity developed with K_2CO_3 was less than that with KOH (e.g., 0.24 vs. 0.68 cm^3/g for activation at 800°C with a K_2CO_3 to carbon mass ratio of 2). The morphology after activation with K_2CO_3 was more similar to the raw petcoke (compare Figure S5c,l) than after activation with KOH (Figures 3H and S5f). Nonetheless, sulphur was removed after activation with K_2CO_3 with ∼1 wt.% remaining (Figure S5, Table 1). Essentially no sulphur was removed and no porosity developed after
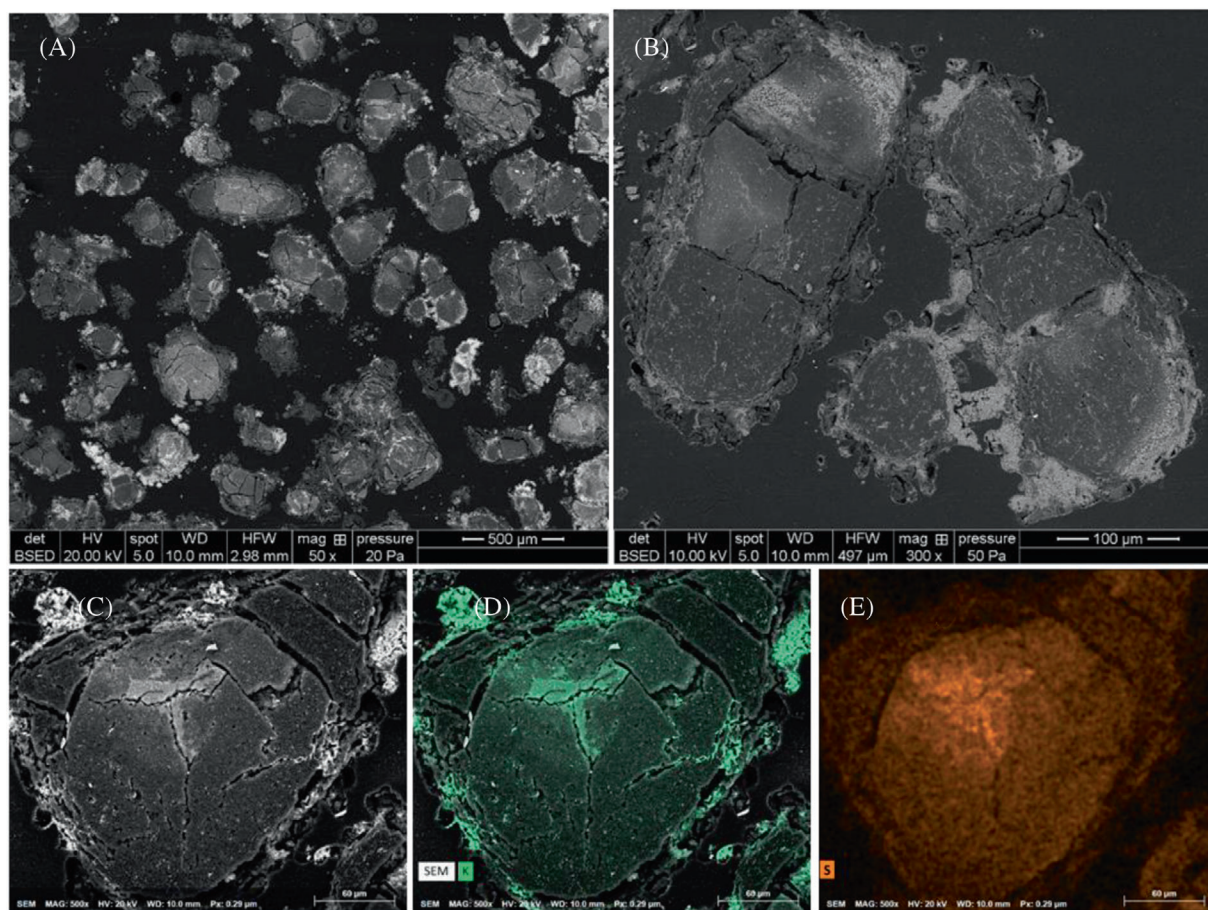
FIGURE 5 Scanning electron microscopy (SEM) analysis of polished samples of petcoke activated with KOH but not washed; (A–C) different magnifications of the sample, (D) potassium mapping, and (E) sulphur mapping. Petcoke activated with a KOH to carbon mass ratio of 2 at 800°C

activation with Na_2CO_3 at 800°C. The hydroxide activation agents have pure component fusion temperatures of 360°C for KOH and 320°C for NaOH, which are lower than those of the corresponding carbonate activation agents—891°C for K_2CO_3 and 851°C for Na_2CO_3.[38] As shown in Figures 4 and 5, a molten layer was formed after activation with the hydroxide species. Thermodynamic calculations by Yuan et al.[18] reported that at ~400°C starting with an initial KOH to carbon ratio of 2, the equilibrium percentage of potassium as potassium carbonate is ~20 mol%. This composition corresponds to a liquid phase according to the KOH/K_2CO_3 phase diagram.[27]

As activation proceeds, however, the hydroxide species will be converted to carbonate species (Reactions (1) and (2)). Furthermore, CO produced in Reaction (2) reacts with the hydroxide species as shown in Reaction (4):

$$CO + 2MOH \rightarrow H_2 + M_2CO_3 \qquad (4)$$
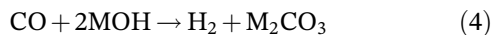
The carbonate species is more stable than the hydroxide species, and the activation rate will slow as this

conversion reaction proceeds. In addition, the increased proportion of carbonate may result in solidification of the chemical phase. The KOH/K_2CO_3 phase diagram[27] indicates that, as the fraction of KOH decreases to 0.2, the mixture will solidify at 800°C. As many other species besides KOH and K_2CO_3 are present during the activation of petcoke, this composition is only an estimate.

The pore volume and surface area of petcoke measured by CO_2 adsorption are 0.01 cm³/g and 40 m²/g, respectively. The diameters of OH^-, K^+, and Na^+ ions are 0.220,[39] 0.203, and 0.166 nm, respectively, and, thus, these species could migrate throughout the particles and catalyze the breaking of the C—S bonds in petcoke. According to the products of the reaction, Utz et al.[40] inferred that the C—S bond undergoes homolysis in the presence of the hydroxides at 375°C to generate a free radical, which can be capped by hydrogen or through polymerization, releasing the sulphur as a sulphide or sulphate species.[12–14] The sulphur released from petcoke during activation reacts with the alkali ions to form Na_2S, K_2S, Na_2SO_4, and K_2SO_4, which have (pure

FIGURE 7 Yield versus pore volume developed for petcoke activated with (A) KOH (▲) or K_2CO_3 (●), and (B) NaOH (■) with chemical agent to carbon ratios from 0.5 to 5 at different temperatures. Dashed lines represent maximum possible pore volume developed by burn-off or intercalation of K or Na
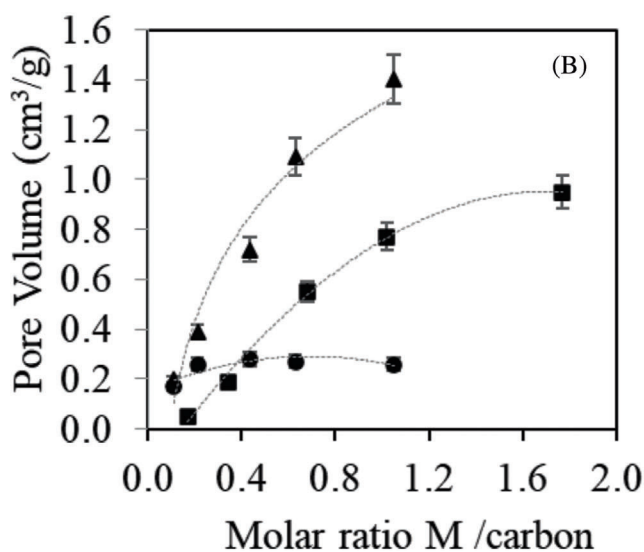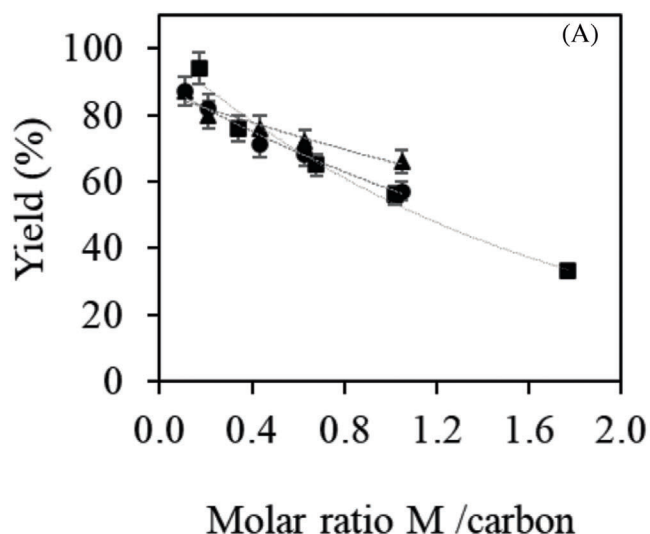

FIGURE 6 Impact of alkali metal, M, to carbon molar ratio (where M is K or Na) on (A) yield and (B) pore volume of petcoke activated at 800°C with NaOH (■), KOH (▲), and K_2CO_3 (●)

component) fusion temperatures of 1176, 840, 884, and 1069°C, respectively, but these sulphur species are soluble in molten hydroxides.[27]

Plotting the yield versus the metal (M representing K or Na) to carbon molar ratio illustrates that the yields decreased from ∼95% to ∼60% as the ratio increased from ∼0.1 to 1, with slightly higher yields obtained when using KOH rather than NaOH or K_2CO_3 (Figure 6A). The resulting pore volumes were highly dependent on the molar ratio for activation with KOH and NaOH, and highest for KOH, then NaOH, and finally K_2CO_3 (Figure 6B). Because the yields were similar, but the pore volumes were not, burn-off or combustion of the carbon was not the only mechanism by which porosity was created.
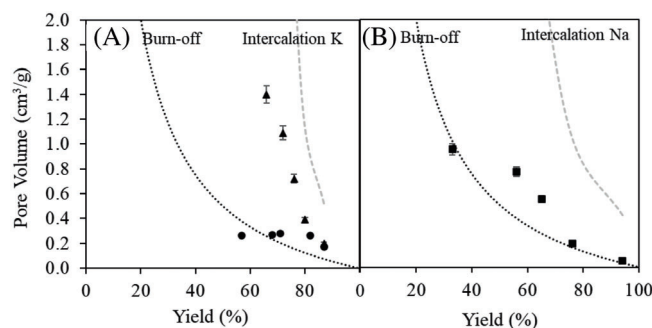
The theoretical pore volumes for complete burn-off and complete intercalation of K or Na as a function of yield were determined and are plotted in Figure 7. For activation with KOH, the actual pore volumes and yields are between the theoretical lines for complete intercalation and complete burn-off, regardless of the KOH to carbon ratio and reaction temperature. For activation with NaOH, the data are closer to the complete burn-off curve. For K_2CO_3, a constant pore volume developed regardless of the amount of activation agent used. This result is consistent with K_2CO_3 not melting during activation, and there being minimal interaction between the activation agent and the carbon. Pore development was limited (∼0.25 cm³/g) but the particles were consumed from the outside (decreasing yield with increased amount of chemical reagent).

The surface tension of Na is nearly double of that of K within a temperature range of 300 to 800°C; at 800°C, the surface tensions are 65 and 125 dynes/cm for K and Na, respectively. The lower mobility of Na is consistent with larger pores forming (Figure S1) relative to those formed with K and the yields being closer to those predicted by burn-off than intercalation (i.e., the particles being consumed preferentially over porosity development within the particles). In addition, if pore volume developed is related to intercalated/inserted M, the volume of K and Na influence the final pore volume. The density of K and Na are 0.665 and 0.73 g/cm³ at 800°C, which is consistent with larger pore volumes obtained with KOH activation (that is, the lower the density the higher the pore volume). Moreover, sulphur was present throughout the particles, which when removed by washing would contribute to the final pore volume.

In summary, the activation process includes the following steps. First, the metal hydroxide (KOH or NaOH) melts, forming a molten layer over the petcoke

particles.[26] The alkali species (molecules or ions) diffuse into the particle, catalyzing C—S bond breakage[12] between 400–600°C throughout the particles. The liberated sulphur reacts to form inorganic salt species (M_2S, M_2SO_4, and/or sulphur species with the ash, which may be dissolved in the molten phase) or gas phase species (H_2S and SO_2). As the temperature increases, the molten MOH gasifies some carbon while other species, such as M_2CO_3, M_2O, and M, form. Some molten species may intercalate or insert into the carbon structure. Note that there is no direct evidence for intercalation, but indirectly, more pore volume was created than could be accounted for by gasification/burn-off alone. After the sample is cooled and the chemical species are washed away, a porous AC remains.

4 | CONCLUSION

In this study, petcoke was activated with different chemical agents by heating in flowing nitrogen to 400–800°C. The obtained porosities and yields obtained under different conditions were related to the phase behaviour of the species present. In particular, potassium and sodium hydroxide have lower fusion temperatures than their carbonate counterparts, and thus are better activation agents. When a molten phase formed, there was better contact between the activation agent and the carbon substrate, promoting the breaking of the C—S bonds. Electron microscopy images of the cross-sections of activated particles confirmed that the majority of the sulphur remained in the petcoke before washing, and that potassium from KOH penetrated to the core of the particles (90–150 μm). Activation with steam further confirmed that porosity was created throughout the particles. Based on the yields and porosities obtained, gasification was not the only mechanism for pore formation.

AUTHOR CONTRIBUTIONS

Vicente Montes: Conceptualization; funding acquisition; investigation; validation; writing – original draft; writing – review and editing. **Ye Xiao:** Data curation; formal analysis; writing – review and editing. **Jingfeng Wu:** Investigation; writing – review and editing. **Josephine M. Hill:** Conceptualization; funding acquisition; methodology; project administration; resources; writing – review and editing.

DATA AVAILABILITY STATEMENT

The data that supports the findings of this study are available in the supplementary material of this article.

ORCID

Vicente Montes https://orcid.org/0000-0002-1851-3758
Josephine M. Hill https://orcid.org/0000-0003-2708-565X

REFERENCES

[1] A. O. Wennerberg, T. M. O'Grady, *US Patent 4,082,694*, **1978**.
[2] C. Ma, R. Wang, Z. Xie, H. Zhang, Z. Li, J. Shi, *J. Porous Mater.* **2017**, *24*, 1437.
[3] J. Romanos, M. Beckner, T. Rash, L. Firlej, B. Kuchta, P. Yu, G. Suppes, C. Wexler, P. Pfeifer, *Nanotechnology* **2012**, *23*, 15401.
[4] Y. Zou, B. X. Han, *Adsorpt. Sci. Technol.* **2001**, *19*, 59.
[5] P. González-García, *Renewable Sustainable Energy Rev.* **2018**, *82*, 1393.
[6] A. Linares-Solano, D. Lozano-Castello, M. A. Lillo-Ródenas, D. Cazorla-Amoros, *Chemistry and Physics of Carbon*, Vol. 30, CRC Press, Boca Raton, FL **2008**, p. 1.
[7] K. Chen, W. Li, B. W. Biney, Z. Li, J. Shen, Z. Wang, *RSC Adv.* **2020**, *10*, 40329.
[8] W. Wu, X. Zhang, J. Yang, J. Li, X. Li, *Carbon Letters* **2020**, *30*, 627.
[9] P. V. Kugatov, B. S. Zhirnov, *Chem. Technol. Fuels Oils* **2020**, *56*, 352.
[10] D. Mandal, P. L. Mahapatra, R. Kumari, P. Kumbhakar, A. Biswas, B. Lahiri, A. Chandra, C. S. Tiwary, *Emergent Mater.* **2021**, *4*, 531.
[11] N. A. Rashidi, S. Yusup, *J. Hazard. Mater.* **2021**, *403*, 123876.
[12] J. Shan, J. J. Huang, J. Z. Li, G. Li, J. T. Zhao, Y. T. Fang, *Fuel* **2018**, *215*, 258.
[13] F. Liu, W. Li, H. Chen, B. Li, *Fuel* **2007**, *86*, 360.
[14] J. H. Cai, E. Morris, C. Q. Jia, *J. Sulfur Chem.* **2009**, *30*, 555.
[15] S. H. Lee, C. S. Choi, *Fuel Process. Technol.* **2000**, *64*, 141.
[16] H. Marsh, F. R. Reinoso, *Activated Carbon*, Elsevier Science & Technology Books, Amsterdam, The Netherlands **2006**, p. 536.
[17] Y. Yamashita, K. Ouchi, *Carbon* **1982**, *20*, 47.
[18] M. Yuan, Y. Kim, C. Q. Jia, *Can. J. Chem. Eng.* **2012**, *90*, 1472.
[19] M. A. Lillo-Ródenas, D. Cazorla-Amoros, A. Linares-Solano, *Carbon* **2003**, *41*, 267.
[20] M. A. Lillo-Ródenas, J. Juan-Juan, D. Cazorla-Amoros, A. Linares-Solano, *Carbon* **2004**, *42*, 1371.
[21] W. Wang, S. Xu, K. Wang, J. Liang, W. Zhang, *Fuel Process. Technol.* **2019**, *189*, 74.
[22] E. Raymundo-Piñero, P. Azaïs, T. Cacciaguerra, D. Cazorla-Amoros, A. Linares-Solano, F. Béguin, *Carbon* **2005**, *43*, 786.
[23] Z. Tai, Q. Zhang, Y. Liu, H. Liu, S. Dou, *Carbon* **2017**, *123*, 54.
[24] T. Otowa, R. Tanibata, M. Itoh, *Gas Sep. Purif.* **1993**, *7*, 241.
[25] C. Lu, S. Xu, C. Liu, *J. Anal. Appl. Pyrolysis* **2010**, *87*, 282.

[26] J. Wu, V. Montes, L. D. Virla, J. M. Hill, *Fuel Process. Technol.* **2018**, *181*, 53.

[27] E. M. Levin, C. R. Robbins, H. F. McMurdie, *Phase Diagrams for Ceramists*, American Ceramic Society, Columbus, OH **1964**.

[28] M. Wu, Q. Zha, J. Qiu, X. Han, Y. Guo, Z. Li, A. Yuan, X. Sun, *Fuel* **2005**, *84*, 1992.

[29] J. Choi, Z. G. Barnard, S. Zhang, J. M. Hill, *Can. J. Chem. Eng.* **2012**, *90*, 631.

[30] J. M. Hill, A. Karimi, M. Malekshahian, *Can. J. Chem. Eng.* **2014**, *92*, 1618.

[31] A. Karimi, O. Thinon, J. Fournier, J. M. Hill, *Can. J. Chem. Eng.* **2013**, *91*, 1491.

[32] O. J. Foust, *Sodium NaK Engineering Handbook. Volume I. Chemistry and Physical Properties*, US Atomic Energy Commission, Washington, DC **1972**.

[33] D. Lozano-Castelló, M. A. Lillo-Ródenas, D. Cazorla-Amorós, A. Linares-Solano, *Carbon* **2001**, *39*, 741.

[34] M. A. Lillo-Ródenas, D. Lozano-Castelló, D. Cazorla-Amorós, A. Linares-Solano, *Carbon* **2001**, *39*, 751.

[35] X. Qiao, T. S. Chung, W. F. Guo, T. Matsuura, M. M. Teoh, *J. Membr. Sci.* **2005**, *252*, 37.

[36] L. C. Edwards, K. J. Neyrey, L. P. Lossius, *Essential Readings in Light Metals,* Springer, New York **2016**, p. 130.

[37] A. Karimi, M. R. Gray, *Fuel* **2011**, *90*, 120.

[38] R. Ray, V. Dayal., *Trans. Faraday Soc.* **1936**, *32*, 741.

[39] Y. Marcus, *J. Chem. Phys.* **2012**, *137*, 154501.

[40] B. R. Utz, S. Friedman, S. K. Soboczenski, *Fossil Fuels Utilization*, Vol. 319, American Chemical Society, Washington, DC **1986**, p. 5.

SUPPORTING INFORMATION

Additional supporting information can be found online in the Supporting Information section at the end of this article.